

# Conditional deletion of CB1 receptor in parvalbumin-expressing GABAergic neurons results in partial hearing loss and abnormal auditory brainstem response in mice

Hao-Nan Wu<sup>1</sup>, Tian-Rong Hang<sup>1</sup>, Fang-Fang Yin<sup>2</sup>, Xiao-Tao Guo<sup>3</sup>, Chun-Chen Pan<sup>3</sup>, Jia-Qiang Sun<sup>3</sup>, Jing-Wu Sun<sup>3</sup>, Wei Shi<sup>4</sup>, Qing-Yin Zheng<sup>5</sup>, Chen Lin<sup>6</sup>, and Zheng-Quan Tang<sup>1</sup>

<sup>1</sup>Anhui University

<sup>2</sup>Hefei Comprehensive National Science Center

<sup>3</sup>The First Affiliated Hospital of USTC

<sup>4</sup>Beihang University

<sup>5</sup>Case Western Reserve University

<sup>6</sup>University of Science and Technology of China

October 17, 2024

## Abstract

Cannabinoid receptor 1 (CB1R) is widely expressed in central auditory system and play important roles in synaptic plasticity and sensory processing. However, the function of CB1R in specific neuronal subtypes in the central auditory system is largely unclear. In the current study, we investigated whether CB1R deficiency in the parvalbumin (PV)-expressing interneurons, a major class of GABAergic interneurons, affect hearing function. We first systematically examined the neuronal localization and distribution of CB1R in mice central auditory system using double-label immunofluorescence and confocal laser scanning microscopy, and found that CB1R showed a wide distribution in the central auditory system, especially highly expressed in the cochlear nucleus (CN), superior olivary complex (SOC) and lateral lemniscus (LL). Furthermore, we established a CB1R conditional knockout mice specifically in PV interneurons, and measured auditory function using the auditory brainstem response (ABR) test. Surprisingly, analysis of ABR indicated that conditional deletion of CB1R specifically from PV interneurons significantly elevated the physiological hearing threshold, prolonged the latency of I waves, and decreased the amplitudes of I–V waves. Collectively, these results indicate that CB1R is highly expressed in CN and SOC, as well as deleting CB1R specifically from PV interneurons resulted in partial hearing loss and abnormal brainstem response. Our finding provides an anatomical basis for further investigating CB1R's function in auditory system, and suggest that CB1R expression in inhibitory PV interneurons is essential for hearing function.

# **Conditional deletion of CB1 receptor in parvalbumin-expressing GABAergic neurons results in partial hearing loss and abnormal auditory brainstem response in mice**

Hao-Nan Wu <sup>a,b,1</sup>, Tian-Rong Hang <sup>a,b,1</sup>, Fang-Fang Yin <sup>c</sup>, Xiao-Tao Guo <sup>d</sup>, Chun-Chen Pan <sup>d</sup>, Jia-Qiang Sun <sup>d</sup>, Jing-Wu Sun <sup>d</sup>, Wei Shi <sup>e</sup>, Qing-Yin Zheng <sup>f</sup>, Lin Chen <sup>g</sup> and Zheng-Quan Tang <sup>a,b,d\*</sup>

<sup>a</sup> School of Life Sciences, Anhui University, Hefei, 230601, China.

<sup>b</sup> Key Laboratory of Human Microenvironment and Precision Medicine of Anhui Higher Education Institutes, Anhui University, Hefei, 230601, China.

<sup>c</sup> Anhui Province Key Laboratory of Biomedical Imaging and Intelligent Processing, Institute of Artificial Intelligence, Hefei Comprehensive National Science Center, Hefei 230088, China.

<sup>d</sup> Department of Otolaryngology Head and Neck Surgery, The First Affiliated Hospital of USTC, Division of Life Sciences and Medicine, University of Science and Technology of China, Hefei, 230001, Anhui, China.

<sup>e</sup> Key Laboratory for Biomechanics and Mechanobiology of Ministry of Education, School of Engineering Medicine, Beihang University, Beijing 100083, China.

<sup>f</sup> Department of Otolaryngology-HNS, Case Western Reserve University, Cleveland, Ohio, USA.

<sup>g</sup> Auditory Research Laboratory, University of Science and Technology of China, Hefei 230027, China.

<sup>1</sup> These authors contributed equally.

---

Number of Text Pages: 22

Number of words in Abstract: 230

Number of words in Main Text: 6872

Number of Figures: 4

## **\* Corresponding authors at:**

Zheng-Quan Tang, PhD, Life Science Building, Anhui University, Hefei City 230601, China;

*E-mail address:* [zqtang@ahu.edu.cn](mailto:zqtang@ahu.edu.cn)

## **Abstract**

Cannabinoid receptor 1 (CB1R) is widely expressed in central auditory system and play important roles in synaptic plasticity and sensory processing. However, the function of CB1R in specific neuronal subtypes in the central auditory system is largely unclear. In the current study, we investigated whether CB1R deficiency in the parvalbumin (PV)-expressing interneurons, a major class of GABAergic interneurons, affect hearing function. We first systematically examined the neuronal localization and distribution of CB1R in mice central auditory system using double-label immunofluorescence and confocal laser scanning microscopy, and found that CB1R showed a wide distribution in the central auditory system, especially highly expressed in the cochlear nucleus (CN), superior olivary complex (SOC) and lateral lemniscus (LL). Furthermore, we established a CB1R conditional knockout mice specifically in PV interneurons, and measured auditory function using the auditory brainstem response (ABR) test. Surprisingly, analysis of ABR indicated that conditional deletion of CB1R specifically from PV interneurons significantly elevated the physiological hearing threshold, prolonged the latency of I waves, and decreased the amplitudes of I–V waves. Collectively, these results indicate that CB1R is highly expressed in CN and SOC, as well as deleting CB1R specifically from PV interneurons resulted in partial hearing loss and abnormal brainstem response. Our finding provides an anatomical basis for further investigating CB1R's function in auditory system, and suggest that CB1R expression in inhibitory PV interneurons is essential for hearing function.

**Keywords:** Cannabinoid receptor 1, PV interneurons, Distribution patterns, Conditional knockout, ABR test

## 1. Introduction

The cannabinoid receptor type 1 (CB1R), one of most abundantly expressed G protein-coupled receptors, is highly expressed throughout the central nervous system (CNS) in excitatory and inhibitory neurons, primarily located in presynaptic terminals and preterminal axon segments (1–5). Functionally, activations of CB1R appear to be depolarization dependent presynaptic modulation of neurotransmitter release primarily via Gi/o protein, subsequently modulate neuronal activity, and thus impact a myriad of physiological functions, such as anxiety, stress, learning, memory, cognitive and sensory processing (2,6–8).

Accumulating evidence indicate that CB1R is expressed in central auditory system of several species and modulates synaptic function (9–14). For instance, the expression of CB1R within auditory pathway has been investigated in early 1991 by autoradiographic, and the signals for CB1R in two subregions of cochlear nuclei is consistent with the later spatial distribution studies through immunohistochemistry (10,12,13). Zheng et al. demonstrated that CB1R is expressed in glutamatergic neurons in cochlear nucleus (CN) (14). More recently, Alejandro et al. found that CB1R is expressed in CN, inferior colliculus (IC) and auditory cortex (AC) in the hamster through RT-qPCR and immunostaining (15). Chou et al. found that CB1R is expressed in AC of human and non-human primate (9). Liu et al. investigated the transcriptional abundance of *cnr1* (CB1R encoding gene) mRNA in the brains from adult C57BL/6J mice of two sexes using RNAscope in situ hybridization (ISH) (11), and found expression of CB1R in the IC and AC. Although the expression of CB1R in the central auditory system has been extensively studied, its spatial distribution in the central auditory system brain remains incomplete. Therefore, identification of the distribution pattern of CB1R within the central auditory system is essential to increase our insight into its function.

Although CB1R exists ubiquitously in CNS, the specific function of CB1R depends on the context of cell types, particular in cell types of GABAergic neurons (2,8,16–18). For instance, Busquets-Garcia, A. et al found that CB1R expressed on specific subpopulations of hippocampal GABAergic interneurons plays a key role in the formation of incidental associations and learning (16,17). Recently, Barna Dudok et al. found that the selective expression of CB1R at synapses of CCK-expressing interneurons modulates place cell firing activity and shapes hippocampal spatial representation (1). In the central auditory system, the synaptic location of CB1R in CN was also confirmed using electron microscopy to show its expression in GABAergic terminals (10,13). In addition, the activation of CB1R in the IC can influence GABAergic neurons to modulate motor behavior like haloperidol-induced catalepsy (19). These findings provide a basis for understanding CB1 in physiological functions, and imply the potential role of CB1R in tuning auditory function via influencing GABAergic signaling. However, the roles of CB1R in GABAergic inhibitory interneurons is poorly understood.

Dysregulation of CB1R in the central auditory system is implicated in tinnitus (20–25). Therefore, CB1R provides an excellent opportunity for therapeutic interventions (21). Currently, there has been increasing interest in the use of cannabinoid compounds for the treatment of tinnitus. It was reported the cannabinoids such as tetrahydrocannabinol (THC) and cannabidiol (CBD) that activated CB1R were used for the treatment of tinnitus (26,27). For its promising future in clinic application, CB1R was under popular researches on structure and bio-

pharmacology to investigate how it was featured as a therapeutic target for its interaction with cannabinoids or the analogous ligands (28–31). In addition, animal studies have suggested that downregulation of GABAergic inhibition, particularly parvalbumin (PV) interneurons mediated inhibition in the central auditory system, is implicated in the generation or perception of tinnitus (32,33). Therefore, understanding the physiological roles of CB1R in GABAergic inhibitory interneurons in the central auditory system may provide an insight into mechanisms underlying tinnitus.

To address these questions, we systematically characterized the neuronal localization and distribution of CB1R in mice central auditory nuclei, including CN, SOC, IC, lateral lemniscus (LL), medial geniculate body (MGB) and AC using fluorescence immunohistochemical techniques; we also established a CB1R conditional knockout mice specifically from PV interneurons, as a major type of GABAergic interneurons in the central auditory system, and explored whether deleting CB1R in PV interneurons affect hearing function using auditory brainstem response (ABR) tests. We found that CB1R is highly expressed in the in the CN, SOC and LL. Interestingly, PV interneuron specific deletion of CB1R resulted in partial hearing loss and abnormal auditory brainstem response. This work provides an increasing insight into the potential roles of CB1R in physiological and pathological brain functions, and more insights into the CB1R as a pharmaceutical target in the treatment of tinnitus.

## **2. Materials and Methods**

### **2.1 Animals**

Two types of C57BL/6J transgenic mice, *Cnr1<sup>flox/flox</sup>* and *PV-Cre;Cnr1<sup>flox/flox</sup>* were used for experiments, and they were bred and housed under the guidelines of Institutional Animal Care and Use Committee of Anhui University (IACUC, AHU). The genotyping of these transgenic mice was performed using PCR and agarose gel electrophoresis with primers listed in Table S1, so as to roughly identify a homozygous and a hemizygous mouse. The mice were housed in the facility with controlled temperature and humidity with a 12-hrs light/dark cycle (lights on 8 a.m.) until they were 8~10 weeks old, and food and water were provided ad libitum.

### **2.2 Immunostaining**

Mice were anesthetized with pentobarbital sodium (60 mg/kg body weight, intraperitoneal injection), then transcardially perfused with phosphate buffered saline (0.01 M PBS, pH 7.4) followed by 4% formaldehyde (PFA) prepared at 4 °C to fix the tissues. The brain was extracted and fixed in 4% PFA for further 12 hours before changed to 15% sucrose (in 0.01 M PBS, pH 7.4) for one day and 30% sucrose for another two days at 4 °C successively. Then, the brain was coronal sectioned into 40 μm slices collected in PBS using cryostat microtome (Leica CM 1900, Leica Biosystems, Wetzlar, Germany). These brain sections were permeabilized in a blocking solution (5% goat serum, 0.5% Triton X-100, and 0.01% sodium azide in 0.01 M PBS) for 1 hr at RT, and subsequently incubated with primary antibody against CB1R (1:5000, sc-518035, Santa Cruz) or parvalbumin (1:500, 195002, Synaptic Systems) overnight at 4 °C. All the antibodies were prepared in the blocking solution. After being washed for 10 min in 0.01 M PBS, thrice, the sections were incubated with a secondary antibody goat anti-mouse (Alexa

Fluor 488, 1:250, 33206ES60, Yeasen) or goat anti-rabbit (Alexa Fluor 594, 1:300, 33112ES60, Yeasen) for 2 hours at RT. Finally, the tissues were washed for several times in PBS, then mounted, dried and counterstained with 4',6-diamidino-2-phenylindole (DAPI, BMU107-CN, Abbkine) before cover-slipped. For double-staining, the sections were incubated with individual primary antibody, and revealed with respective secondary antibodies. Fluorescence signal from the sections were captured with a confocal laser scanning microscope (LSM980, Zeiss), and its intensity indicating the expression of proteins was quantitatively or quantitatively analyzed by ImageJ software (NIH). Part of the images were merged for analysis of co-localization of CB1R with PV. Antibodies are listed in Table S2.

### 2.3 Western Blot analysis

The C57BL/6J transgenic mice were sacrificed and used for the immunoblot after anesthesia. Brain tissues were extracted and lysed using homogenizer in ice-cold lysis buffer (20 mM Tris, pH 7.5, 150 mM NaCl, 1% Triton X-100) supplemented with protease inhibitor AEBSF and reductant  $\beta$ -ME. The lysate was centrifuged twice at 15,000 $\times$ g for 20 min at 4 °C to remove insoluble debris, and the supernatant was transferred to a sterile EP-tube for another 20 min centrifugation. The concentration of total proteins in solubilized fractions was determined by Bradford assay using spectrophotometer at 595 nm. Then the protein samples were mixed with 5 $\times$ Loading buffer (Dithiothreitol contained) and denatured in Block Heater for separation by 15% SDS-PAGE (Tanon Electrophoresis System). Separated proteins were transferred onto 0.22  $\mu$ m PVDF membranes individually, and the membranes were blocked in TBST (20 mM Tris-HCl, pH 7.6, 150 mM NaCl, 0.05% Tween 20) with 5% non-fat milk contained for 1 hour at RT. The primary antibodies used for target and reference proteins were anti-CB1R (1:5000, sc-518035, Santa Cruz) and anti-GAPDH (1:5000, AF7021, Affinity) respectively, and they were further detected with HRP-linked secondary antibodies for ECL assessment (Table S2). The blotting bands were visualized with chemiluminescence imaging system (JS-1070P, Peiqing). Band intensities were quantified through ImageJ software (NIH) to analyze the protein expression of CB1R relative to GAPDH in the same sample.

### 2.4 RT-qPCR

Brain tissues isolated from mice were homogenized in Trizol, and then mixed with chloroform for 2 min of shaking and 3 min of quiescence at RT to extract total RNA. The mixture was centrifuged at 12,000 $\times$ g for 15 min at 4 °C to separate water-organic phases. Then the water phase was preserved with isopropyl alcohol added and mixed well before precipitation at -80 °C for 2 hrs. The new mixture was centrifuged for another 15 min at 12,000 $\times$ g to precipitate RNA, and then washed by ice-cold 80% ethanol. Finally, the gelatinoid RNA precipitant was desiccated and dissolved in 0.1% DEPC ddH<sub>2</sub>O. Concentration measurement by OneDrop spectrophotometry (OD1000+, WINS) combined with integrity detection through agarose gel electrophoresis were conducted to evaluate the quality of RNA. Reverse-transcription and quantitative real-time PCR were subsequently performed using the cDNA Synthesis Kit (11141ES60, YEASEN) and qPCR Kit (11184ES08, YEASEN) respectively. Data from qPCR were normalized with the method of  $2^{-\Delta\Delta C_t}$ , and the relative transcription of *cnr1* was derived from the transcript ratio of *cnr1* to  $\beta$ -actin, the reference gene.

All the reagents and materials used were RNase-free, and the primers used to amplify the target genes are shown in Table S1.

## 2.5 Auditory brainstem response (ABR) test

Since the ABR test provides auditory information of nuclei in the central pathway to sound stimulation, a TDT (Tucker Davis Technologies) RZ6 system was used to collect evoked auditory signals of mice. The mice were anesthetized with pentobarbital sodium (60 mg/kg, IP injection) and positioned 10 cm from the free-field speaker (monaural) on a non-electric heating pad (~37 °C) with three platinum coated electrodes placed in the scalp, within the sound-proof chamber. The impedance was adjusted below 5 Ohm before recording, and sound stimuli is produced through the speaker. For click stimulus, the mouse is presented with a wide spectrum click (0.1 ms) in a gradient descent of 10 dB SPL from 90 to 10 dB SPL. Each data point acquisition was repeated for 512 times and the integral signals were averaged for display. For frequency-specific tone burst stimulus, five frequencies including 4, 8, 16, 24 and 32 kHz (0.1 ms) were presented in decreasing levels between 90~20 dB SPL, and each new stimulus was recorded 5 dB SPL down from the previous. Each point of measurement was recorded 512 times to be averaged. ABR threshold was considered as the lowest intensity of recognizable response for the given set of variables, and all the hearing threshold, latency, waveform, and amplitude of ABR data were determined using BioSigRZ software. When finished recording, the mice had electrode removed and were carefully sent to emergence from anesthesia.

## 2.6 Data analysis

In all the experiments, mice in the age of 8 and 10 weeks were randomly selected as biological replicates to make the study reliable. For western-blot, the darkness of blotting-bands was integrated using ImageJ (NIH). For immunostaining, the images collected from confocal microscopy were processed by ZEN (Zeiss) and for further cell numbering or fluorescent intensity integration in ImageJ. The waveform plots exported from BioSigRZ software in ABR test were line-smoothed by Origin9. Other graphs were prepared in Prism software (GraphPad 9.5.0, La Jolla, CA). Normality of the data was tested using the Shapiro-Wilk normality test. Nonparametric data with multiple comparisons were analyzed by Kruskal-Wallis one-way analysis of variance (ANOVA) followed by Holm's Stepdown Bonferroni procedure for adjusted *p*-values. The Mann-Whitney *t* test was used for comparison between two groups. Data with normal distribution were analyzed by one-way ANOVA with Dunnett's post-test or Tukey's correction for multiple comparisons as described in the figure legends. Values are presented as the average mean ± standard error (SEM) for data that were normally distributed or median and interquartile range for data that were not normally distributed for continuous variables. For all comparison, *p* < 0.05 was considered statistically significant. *p* and *n* represent the value of significance and the number of mice, respectively. Data were analyzed using GraphPad Prism software.

## 3. Results

To gain insight into CB1R functions in inhibitory neural circuits of the central auditory system, we selectively deleted *cnr1* by Cre dependent deletion of loxP flanked exons, which

leads to an unstable protein (6,34).  $Cnr1^{flox/flox}$  mice were mated with PV-Cre mice to generate mice with CB1R cKO specifically from PV interneurons.  $Cnr1^{flox/flox}$  mice were used as controls because they express normal levels of CB1R (Fig. S1). Two different genotypic strains,  $Cnr1^{flox/flox}$  and PV-Cre; $Cnr1^{flox/flox}$ , were identified and were randomly separated into several groups for different purposes.

### 3.1 CB1R is highly expressed in auditory brain stem

In the current study, we first analyzed the distribution and expression of CB1R in the central auditory system of mice. The distribution and expression level of CB1R in different brain regions of central auditory system were qualitatively and quantitatively evaluated using immunostaining through fluorescence's imaging, and coronal sections of auditory nuclei were subjected to immunohistochemical analysis. To elucidate the characteristics of CB1R expression in central auditory system, several nuclei among the auditory pathway from  $Cnr1^{flox/flox}$  mice were detected through immunostaining. The CN was further divided into two subregions, dorsal cochlear nucleus (DCN) and ventral cochlear nucleus (VCN). The VCN also included two parts, anterior VCN (AVCN or VCA) and posterior VCN (PVCN or VCP). For superior olivary complex (SOC), three major nuclei, medial superior olive (MSO), lateral superior olive (LSO) and medial nucleus of the trapezoid body (MNTB) were evaluated. For inferior colliculus (IC), the subregions including external cortex IC (ECIC), dorsal cortex IC (DCIC) and central nucleus IC (CNIC) were examined. Moreover, besides auditory cortex (AC), the lateral lemniscus (LL) as well as medial geniculate body (MGB) were also investigated.

From an overall perspective, the CB1R is distributed throughout the central auditory system, including CN, SOC, LL, IC, MGB and AC (Fig. 1a). CB1R proteins were abundantly enriched in CN, SOC and LL, especially in the subregion of VCN when compared to DCN, with the AVCN owned much higher expression than PVCN (Fig. 2a). This was consistent with the immunohistochemistry result of CN that reported by Zheng et al., previously (14). In SOC, the CB1R proteins were expressed stably with a similar strength in MSO, LSO and MNTB (Fig. 2a). Moreover, the CB1R proteins were also detected in MGB, with a moderate expression level relative to other three regions (Fig. 1a). In contrast, the expression of CB1R in IC and AC were poorly detected for the weak fluorescence signals, particularly it was almost invisible for any positive immunoactivity of CB1R in AC (Fig. 1a). Intriguingly, the IC nucleus showed a weak expression of CB1R, the fluorescence signals were also found sporadically distributed in the subregions of DCIC and CNIC (Fig. 2a).

The distribution of CB1R proteins within different regions were qualitatively and quantitatively evaluated through number counting as well as fluorescence intensity integration of CB1R positive neurons (Fig. 1b, 1c and Fig. 2b, 2c). For each nucleus, three to five coronal sections with different distances from the bregma were used for statistics, so as to cover the overall brain region. Partially in agreement with the megascopic observation, the total numbers of CB1R positive neurons were significantly higher in the regions of SOC and LL, when compared with others (Fig. 1b). Among all the auditory regions, the number of CB1R<sup>+</sup> neurons in CN took the second place when IC with fewer CB1R<sup>+</sup> neurons than SOC, LL and CN, although CN seemed to have a certain high expression of CB1R proteins. For MGB and AC,

much fewer numbers of CB1R<sup>+</sup> neurons were identified due to the expression level of CB1R proteins were relative lower in these two regions (Fig. 1b).

To quantify the CB1R expression patterns more accurately, the average fluorescence intensities of CB1R among distinct nuclei were integrated for comprehensive analysis (Fig. 1c, 2b). Compared with the cell number calculated above, the statistic of average fluorescence intensities demonstrated that the CB1R were maximumly distributed in the regions of SOC and CN (Fig. 1c). While cell numbers in LL were almost the same as in SOC, the average expression intensity of CB1R proteins indicated by fluorescence signal within LL was closer to the value from CN (Fig. 1c). Among the subregions of SOC where had most abundant expression of CB1R, when a greater number of CB1R<sup>+</sup> neuron was detected in LSO than MNTB and MSO, the average fluorescence intensities were similar in three nuclei (Fig. 2b, 2c). This inconsistency of two kinds of statistics was also observed in subregions of CN or IC (Fig. 2b, 2c). The discrepancy between analysis of cell number and fluorescence intensity might be attributed to the different enrichment of CB1R expression within distinct brain regions or cell types, as well as the differentiated distribution of CB1R or CB1R<sup>+</sup> neurons within specific region.

### 3.2 CB1R knockout decreases the distribution of CB1R<sup>+</sup> PV-neurons

In order to confirm that deleting CB1R specifically from PV neurons, the double-staining of CB1R and PV as well as their co-localization in PV-Cre;Cnr1<sup>fllox/fllox</sup> and Cnr1<sup>fllox/fllox</sup> mice were conducted (Fig. 3a, 3b and Fig S5). We found that proteins of PV and CB1R were abundantly distributed in the CN and SOC, they were co-localized in a certain proportion of neurons within these two regions, and the expression of PV was unaffected by Cnr1-cKO, (Fig. 1, 2 and 3). It was not surprised to see that the knockout of *Cnr1* in PV-positive neurons might trigger a noteworthy change of CB1R expression in CN and SOC of PV-Cre;Cnr1<sup>fllox/fllox</sup> mice (Fig. 1, 3). When compared with Cnr1<sup>fllox/fllox</sup> mice, the co-localizations of these two proteins were notably reduced in the PV-Cre;Cnr1<sup>fllox/fllox</sup> group, and the integral levels of CB1R expression were also downregulated for its conditional deficiency (Fig. 3a-c). As expected, the extent of CB1R downregulation that modulated by Cre recombinas integrated in PV positive neurons, was in consistent with the phenomena that observed in ABR tests previously (Fig. 3, 4).

To further confirm the expressional change of CB1R proteins within these specific regions, a western-blot assay together with a real-time quantification PCR test were performed on the KO and non-KO mice (Fig. S6). Only the regions of CN with anatomically marginal definition were exacted scrupulously for both western-blot and qPCR so as to ensure precision of the results (Fig. S6). Moreover, regions of IC and hippocampus were also prepared for RT-qPCR (Fig. S6b). In contrast to Cnr1<sup>fllox/fllox</sup> group, the protein expression level of CB1R from PV-Cre;Cnr1<sup>fllox/fllox</sup> mice were sharply decreased in CN (Fig. S6a). Although there was no significant difference between two transgenic groups when it referred to gene transcription, the entire downtrend of KO mice revealed by mRNA transcripts was consistent with the results from immunostaining and western-blot (Fig. 3, Fig. S6). Overall, our results indicated that deleting CB1R specifically from PV neurons dramatically decreased the distribution of CB1R<sup>+</sup> PV-neurons in the CN and SOC.

### 3.3 CB1R cKO in PV interneurons results in partial hearing loss

The CB1R were presented in many different cell types, with their expression levels dynamically varied amongst distinct subcellular locations (8,16,18,35). CB1R is recognized to have the most abundant expression in GABAergic interneurons, while glutamatergic, glycinergic or other neuronal types with relatively low-to-moderate expression levels of this protein (36). The diversity of GABAergic neurons can be characterized by transcriptomes, morphology and electrophysiology. PV interneurons are one of the most abundant GABAergic neurons in the central auditory system (36,37). Therefore, our results suggest that loss of CB1R in PV-interneurons might produce abnormal hearing function.

To determine whether deleting CB1R in PV-interneurons impact hearing function, we performed auditory brainstem response (ABR) tests and measured the thresholds, latencies of wave I and amplitudes of waves I-IV in PV-Cre;Cnr1<sup>flox/flox</sup> mice and Cnr1<sup>flox/flox</sup> mice. Compared with Cnr1<sup>flox/flox</sup> group, the average hearing thresholds for either clicks or pure-tones in group of PV-Cre;Cnr1<sup>flox/flox</sup> mice slightly shifted (Fig. 4a,b). These increased thresholds for PV-Cre;Cnr1<sup>flox/flox</sup> mice indicated that conditional knockout of CB1R specifically from PV-interneurons resulted in partial hearing loss in mice.

### 3.4 PV-Cre;Cnr1<sup>flox/flox</sup> mice exhibit abnormal auditory brainstem responses

Among the tone-burst with five frequencies (4~32 kHz), the hearing thresholds presented a 'V'-shaped curve to imply the mice with best hearing under 16 kHz (Fig. 4b). Therefore, the ABR waveforms recorded at 90 dB SPL from two transgenic groups were superimposed under stimuli of click as well as 16 kHz (the representative one) (Fig. 4c). Surprisingly, there were significantly differences in ABR wave characteristics between two groups of mice (Fig. 4c-e). The amplitude of wave II for clicks decreased dramatically in PV-Cre;Cnr1<sup>flox/flox</sup> mice when compared to Cnr1<sup>flox/flox</sup>, while the amplitudes of wave I, III, IV and V had a slightly decrease (Fig. 4c, 4e). Both the latencies and amplitudes of the waveforms I-V for 16 kHz pure tones were significantly changed in PV-Cre;Cnr1<sup>flox/flox</sup> mice (Fig. 4c-e, Fig. S3). Especially the wave II and III, the most typical waves that were generally recognized to represent CN and SOC respectively, were drastically changed both in amplitudes and latencies (Fig. S2~S4). The statistics derived from the ABR waveforms of two transgenic mice demonstrated that, except the data collected under 32 kHz were ambiguous for analysis, the amplitudes of wave I~IV for clicks or other frequencies of tone burst were decreased (Fig. S4).

Generally, the PV-Cre;Cnr1<sup>flox/flox</sup> mice exhibited longer latencies and lower amplitudes, suggesting that the transduction velocity and strength of the auditory signal in CB1R cKO specifically in PV-interneuron mice were decreased. Taken together, the increased thresholds, prolonged latencies, and attenuated amplitudes of ABR waves observed in PV-Cre;Cnr1<sup>flox/flox</sup> mice suggested that CB1R deficiency in PV interneurons impair auditory function.

## 4. Discussion

In the current study, we assessed region-specific distribution of the CB1R across the central auditory system of mice using fluorescence immunohistochemical techniques, and

found that CB1R is highly expressed in the CN, SOC and LL. Furthermore, we conditionally deleted CB1R specifically from PV interneurons and found that deletion of CB1R specifically from PV interneurons resulted in partial hearing loss and abnormal auditory brainstem response. Our findings support a functional role for CB1R in regulating inhibitory circuitry function in the central auditory system to ultimately impact auditory processing.

#### **4.1 The distribution of CB1R in the central auditory system**

ECS components and their role in synaptic plasticity and neurodevelopment have been extensively described in numerous studies (10,38). However, few studies have concerned about the intrinsic mapping of CB1R in CNS, especially in central auditory system. While the distribution of *cnr1* transcripts have been detected in several brain regions through RNA scope, more researches concerning the expression characteristic of CB1R proteins is warranted (39,40). Here, our studies systematically evaluated the differentiated expression patterns of CB1R in central auditory system through immunostaining, which is more reliable for protein evaluation than *in situ* hybridization for mRNA transcript detection. We observed the expression of CB1R in the CN, SOC, IC, LL, MGB and AC of mice, which is consistent with the previous studies (13,14,21).

We also found that CB1R is highly expressed in PV interneurons in the several nuclei of auditory system. The functions of CB1R were not only determined by the expression levels in specific neuronal subpopulations, but also related with the downstream efficacy of its G protein-dependent signaling. For instance, although the GABAergic neurons in the hippocampus have much higher CB1R expression levels than the glutamatergic neurons, they had much lower efficacy of G protein-dependent signaling of CB1R shown by the conditional mutant mice lacking CB1R expression in GABAergic or glutamatergic neurons (41). Likewise, although the CB1R was most abundantly expressed in GABAergic interneurons with PV-positive neurons, the capacity of CB1R distinguished by the cell type besides its expression abundance in distinct nuclei should be considered as well (36).

#### **4.2 Functional implications of CB1R in PV-interneurons**

Our findings in this study uncovers an important role of cell type specific CB1R in hearing. The conditional deletion of *cnr1* gene from PV-positive neurons produced a decrease in both cell numbers and protein expression of CB1R. More importantly, the transgenic mice with CB1R deficiency exhibited partial hearing loss and auditory dysfunction revealed by ABR test. There are five identifiable waves in ABR test, labeled as I-V. Wave I represents the summated response from the spiral ganglion and auditory nerve while waves II-V represent responses from the ascending auditory brainstem pathway. Our results demonstrated the transgenic mice with CB1R deficiency in PV-interneurons exhibited the prolongation of waves I latencies, suggesting that auditory nerve-brainstem conduction velocity is decreased. Furthermore, a decrease in the amplitudes of waves I-V observed in the transgenic mice with CB1R deficiency suggest that conditional deletion of CB1R from PV-interneurons resulted in abnormal auditory brainstem function.

The nuclei of SOC were responsible for azimuthal sound location of ILD (interaural level

difference) and ITD (interaural time difference) coding, which could be disrupted by early hearing loss (42). In *Cnr1*-cKO mice, the CB1R-positive neurons and CB1R expression were significantly decreased in SOC, accompanied by the wave II and III that typically represented CN and SOC were drastically changed in ABR tests, respectively. Therefore, the sculpture of CB1R expression patterns would shed light on the importance of CB1R involved in auditory function and dysfunction as a neuromodulator. Although the expression of CB1R was quite low in the regions of MGB and AC, the roles of CB1R in auditory function should be elucidated in the future.

It has been reported that CB1R undergoes extensive trafficking between the cytoplasm and the presynaptic terminals, especially in brain regions where it is quite active (43). This process was dynamically regulated, therefore, the barely visible signal in a certain region detected in immunostaining did not mean that there was no expression of CB1R. In 2020, Zhong's group investigated the intracellular organization of CB1R within the axons of neurons using a structured illumination microscopy with high spatial resolution (44). The CB1R proteins are presented at both presynaptic terminals and postsynaptic compartments of several types of neurons, and they were also found in glial cells such as astrocytes and microglial cells with lower amounts (45). Astrocytes play an important role in modulation of brain homeostasis and synaptic plasticity through the cooperation between astrocytes and neurons, and these functions can be shaped by CB1R (46,47). Moreover, new evidence recently pointed to the presence of CB1R (mtCB1R) at mitochondrial membranes of both presynaptic and somatodendritic compartments of neurons, being associated with brain metabolism, but the specific function not fully understood (46). The ubiquitous expression of CB1R in these components suggest that the CB1R might be involved in various biological processes with functional diversity (40).

Beyond the physiological function of CB1R, our findings may provide insight into the biological mechanisms of tinnitus. The dysfunction of CB1R is implicated in tinnitus, therefore, the cannabinoid receptor CB1R may exert like a drug target for tinnitus. The CN is generally considered as a key region that associated with tinnitus initiation. In 2007, Zheng et al. investigated CB1R expression in the subregions of the CN using immunohistochemistry (14). The morphological cell types of CB1R positive cells are different in DCN and VCN, and the number of CB1R-expressing neurons in VCN are decreased in rats with salicylate-induced tinnitus that confirmed by conditioned behavioral paradigm. In 2011, Jason et al. reported that the DCN is hyperactivated in noise-exposed mice mainly due to decreased GABAergic inhibition, leading to the emergence of tinnitus perception (33). The expression of CB1R and the number of CB1R positive neurons in CN changed in rats with salicylate-induced tinnitus, indicating that the dysfunction of CB1R may be involved in auditory dysfunction. However, the clinical cases that treating tinnitus through cannabinoids or agonists were contradictory, so the mechanisms for CB1R modulation of auditory system remain uncovered. This expression profile of CB1R might increase current understandings of CB1R in central auditory system, and potentially promote the cannabinoid-based drug target finding and drug development of pharmacotherapies for auditory dysfunctions such as tinnitus.

In summary, we demonstrate that selective deletion of CB1R in GABAergic PV cells resulted in a defective inhibitory PV cell circuits in central auditory system, and led to partial

hearing loss and abnormal auditory brain stem response. We tentatively conclude from our data and those deriving from other previous reports that CB1R in PV-interneurons may influence the development and auditory function (1,2,35,38).

### **Declaration of Competing Interest**

The authors declare that the research was conducted in the absence of any commercial or financial relationships that could be construed as a potential conflict of interest.

### **Acknowledgments**

We thank Dr. X. Song, Dr. F. Yin and Dr. D. Bi for providing technical assistance of microscopic imaging, and we thank W. An and Y. Wu for technical assistance in ABR test.

### **Fundings**

This work was supported by the Natural Science Foundation of China (Grants 32271059 and 82071061 to Zheng-Quan Tang; Grant 82271180 to Jing-Wu Sun; grant Z200024 to W.S.; Grants 81970886, 81570915 to Lin Chen) and Anhui Provincial Natural Science Foundation for Youth (grant No. 2008085QC161 to Tian-Rong Hang).

### **Author Contributions**

Zheng-Quan Tang, Tian-Rong Hang, Xiao-Tao Guo, Chun-Chen Pan, Jia-Qiang Sun, Jing-Wu Sun, Wei Shi, Qing-Yin Zheng and Lin Chen provided the scientific direction and the overall experimental design for the studies. Hao-Nan Wu, Tian-Rong Hang, and Fang-Fang Yin performed the molecular experiments, ABR tests and statistical analysis. Hao-Nan Wu, Tian-Rong Hang, Xiao-Tao Guo, Chun-Chen Pan, Jia-Qiang Sun, Jing-Wu Sun, Wei Shi, Qing-Yin Zheng, Lin Chen and Zheng-Quan Tang wrote the manuscript.

## References

1. B D, Lz F, Js F, S M, J H, Dk K, et al. Retrograde endocannabinoid signaling at inhibitory synapses in vivo. *Science (New York, NY)* [Internet]. 2024 Mar [cited 2024 Oct 11];383(6686). Available from: <https://pubmed.ncbi.nlm.nih.gov/38422134/>
2. Barti B, Dudok B, Kenesei K, Zöldi M, Miczán V, Balla GY, et al. Presynaptic nanoscale components of retrograde synaptic signaling. *Sci Adv.* 2024 May 31;10(22):eado0077.
3. Castillo PE, Younits TJ, Chávez AE, Hashimoto Y. Endocannabinoid signaling and synaptic function. *Neuron.* 2012 Oct 4;76(1):70–81.
4. Domenici MR, Azad SC, Marsicano G, Schierloh A, Wotjak CT, Dodt HU, et al. Cannabinoid receptor type 1 located on presynaptic terminals of principal neurons in the forebrain controls glutamatergic synaptic transmission. *J Neurosci.* 2006 May 24;26(21):5794–9.
5. Kendall DA, Yudowski GA. Cannabinoid Receptors in the Central Nervous System: Their Signaling and Roles in Disease. *Front Cell Neurosci.* 2016;10:294.
6. Marsicano G, Wotjak CT, Azad SC, Bisogno T, Rammes G, Cascio MG, et al. The endogenous cannabinoid system controls extinction of aversive memories. *Nature.* 2002 Aug 1;418(6897):530–4.
7. Stachowicz K. Deciphering the mechanisms of reciprocal regulation or interdependence at the cannabinoid CB1 receptors and cyclooxygenase-2 level: Effects on mood, cognitive implications, and synaptic signaling. *Neurosci Biobehav Rev.* 2023 Dec;155:105439.
8. V DG, S R, B L, M H, F R. Cell type-specific genetic reconstitution of CB1 receptor subsets to assess their role in exploratory behaviour, sociability, and memory. *The European journal of neuroscience* [Internet]. 2022 Feb [cited 2024 Oct 15];55(4). Available from: <https://pubmed.ncbi.nlm.nih.gov/33253450/>
9. S C, T R, Kn F, Da L, Ra S. Cell type specific cannabinoid CB1 receptor distribution across the human and non-human primate cortex. *Scientific reports* [Internet]. 2022 Oct 6 [cited 2024 Oct 11];12(1). Available from: <https://pubmed.ncbi.nlm.nih.gov/35688916/>
10. Tzounopoulos T, Rubio ME, Keen JE, Trussell LO. Coactivation of pre- and postsynaptic signaling mechanisms determines cell-specific spike-timing-dependent plasticity. *Neuron.* 2007 Apr 19;54(2):291–301.
11. X L, X L, G Z, F W, L W. Sexual dimorphic distribution of cannabinoid 1 receptor mRNA in adult C57BL/6J mice. *The Journal of comparative neurology* [Internet]. 2020 Aug [cited 2024 Oct 11];528(12). Available from: <https://pubmed.ncbi.nlm.nih.gov/31997354/>
12. Y Z, Me R, T T. Distinct functional and anatomical architecture of the endocannabinoid system in the auditory brainstem. *Journal of neurophysiology* [Internet]. 2009 May [cited 2024 Oct 11];101(5). Available from: <https://pubmed.ncbi.nlm.nih.gov/19279154/>

13. Zhao Y, Rubio M, Tzounopoulos T. Mechanisms underlying input-specific expression of endocannabinoid-mediated synaptic plasticity in the dorsal cochlear nucleus. *Hear Res.* 2011 Sep;279(1-2):67-73.
14. Zheng Y, Baek JH, Smith PF, Darlington CL. Cannabinoid receptor down-regulation in the ventral cochlear nucleus in a salicylate model of tinnitus. *Hear Res.* 2007 Jun;228(1-2):105-11.
15. Fuerte-Hortigón A, Gonçalves J, Zeballos L, Masa R, Gómez-Nieto R, López DE. Distribution of the Cannabinoid Receptor Type 1 in the Brain of the Genetically Audiogenic Seizure-Prone Hamster GASH/Sal. *Front Behav Neurosci.* 2021;15:613798.
16. Busquets-Garcia A, Oliveira da Cruz JF, Terral G, Pagano Zottola AC, Soria-Gómez E, Contini A, et al. Hippocampal CB1 Receptors Control Incidental Associations. *Neuron.* 2018 Sep 19;99(6):1247-1259.e7.
17. Busquets-Garcia A, Bains J, Marsicano G. CB1 Receptor Signaling in the Brain: Extracting Specificity from Ubiquity. *Neuropsychopharmacology.* 2018 Jan;43(1):4-20.
18. Kendall DA, Yudowski GA. Cannabinoid Receptors in the Central Nervous System: Their Signaling and Roles in Disease. *Front Cell Neurosci.* 2016;10:294.
19. P M, Ri de F, Mo S, Nc C, L MT. CB1 cannabinoid receptor-mediated anandamide signaling mechanisms of the inferior colliculus modulate the haloperidol-induced catalepsy. *Neuroscience [Internet].* 2016 Nov 19 [cited 2024 Oct 11];337. Available from: <https://pubmed.ncbi.nlm.nih.gov/27595886/>
20. Hwang JH, Chan YC. Expression of Dopamine Receptor 1A and Cannabinoid Receptor 1 Genes in the Cochlea and Brain after Salicylate-Induced Tinnitus. *ORL J Otorhinolaryngol Relat Spec.* 2016;78(5):268-75.
21. Ji B, B C, S H, Sph A, W O, Ar P, et al. Effects of the cannabinoid CB1 agonist ACEA on salicylate ototoxicity, hyperacusis and tinnitus in guinea pigs. *Hearing research [Internet].* 2017 Dec [cited 2024 Oct 11];356. Available from: <https://pubmed.ncbi.nlm.nih.gov/29108871/>
22. Pf S, Y Z. Cannabinoids, cannabinoid receptors and tinnitus. *Hearing research [Internet].* 2016 Feb [cited 2024 Oct 11];332. Available from: <https://pubmed.ncbi.nlm.nih.gov/26433054/>
23. Y Z, P R, Pf S. Cannabinoid CB1 Receptor Agonists Do Not Decrease, but may Increase Acoustic Trauma-Induced Tinnitus in Rats. *Frontiers in neurology [Internet].* 2015 Mar 18 [cited 2024 Oct 11];6. Available from: <https://pubmed.ncbi.nlm.nih.gov/25852639/>
24. Y Z, Pf S. Cannabinoid drugs: will they relieve or exacerbate tinnitus? *Current opinion in neurology [Internet].* 2019 Feb [cited 2024 Oct 11];32(1). Available from: <https://pubmed.ncbi.nlm.nih.gov/30507635/>

25. Zugaib J, Leão RM. Enhancement of Endocannabinoid-dependent Depolarization-induced Suppression of Excitation in Glycinergic Neurons by Prolonged Exposure to High Doses of Salicylate. *Neuroscience*. 2018 Apr 15;376:72–9.
26. A M, M F, M A, P C, E P, At G, et al. Cannabinoids in the Treatment of Epilepsy: Current Status and Future Prospects. *Neuropsychiatric disease and treatment* [Internet]. 2020 Jul 2 [cited 2024 Oct 11];16. Available from: <https://pubmed.ncbi.nlm.nih.gov/32103958/>
27. Nabbout R, Thiele EA. The role of cannabinoids in epilepsy treatment: a critical review of efficacy results from clinical trials. *Epileptic Disord*. 2020 Jan 1;22(S1):23–8.
28. Jung SW, Cho AE, Yu W. Exploring the Ligand Efficacy of Cannabinoid Receptor 1 (CB1) using Molecular Dynamics Simulations. *Sci Rep*. 2018 Sep 13;8(1):13787.
29. Krishna Kumar K, Robertson MJ, Thadhani E, Wang H, Suomivuori CM, Powers AS, et al. Structural basis for activation of CB1 by an endocannabinoid analog. *Nat Commun*. 2023 May 9;14(1):2672.
30. Leo LM, Abood ME. CB1 Cannabinoid Receptor Signaling and Biased Signaling. *Molecules*. 2021 Sep 6;26(17):5413.
31. R N, Ea T. The role of cannabinoids in epilepsy treatment: a critical review of efficacy results from clinical trials. *Epileptic disorders: international epilepsy journal with videotape* [Internet]. 2020 Jan 1 [cited 2024 Oct 11];22(S1). Available from: <https://pubmed.ncbi.nlm.nih.gov/31916540/>
32. Masri S, Chan N, Marsh T, Zinsmaier A, Schaub D, Zhang L, et al. Chemogenetic Activation of Cortical Parvalbumin-Positive Interneurons Reverses Noise-Induced Impairments in Gap Detection. *J Neurosci*. 2021 Oct 20;41(42):8848–57.
33. Middleton JW, Kiritani T, Pedersen C, Turner JG, Shepherd GMG, Tzounopoulos T. Mice with behavioral evidence of tinnitus exhibit dorsal cochlear nucleus hyperactivity because of decreased GABAergic inhibition. *Proc Natl Acad Sci U S A*. 2011 May 3;108(18):7601–6.
34. Marsicano G, Goodenough S, Monory K, Hermann H, Eder M, Cannich A, et al. CB1 cannabinoid receptors and on-demand defense against excitotoxicity. *Science*. 2003 Oct 3;302(5642):84–8.
35. B G, K X, H M, K R, H X, Nd H, et al. CB1R dysfunction of inhibitory synapses in the ACC drives chronic social isolation stress-induced social impairments in male mice. *Neuron* [Internet]. 2024 Jul 2 [cited 2024 Oct 11];112(3). Available from: <https://pubmed.ncbi.nlm.nih.gov/37992714/>
36. Huang ZJ, Paul A. The diversity of GABAergic neurons and neural communication elements. *Nat Rev Neurosci*. 2019 Sep;20(9):563–72.

37. Hu H, Gan J, Jonas P. Interneurons. Fast-spiking, parvalbumin<sup>+</sup> GABAergic interneurons: from cellular design to microcircuit function. *Science*. 2014 Aug 1;345(6196):1255-263.
38. Clarke TL, Johnson RL, Simone JJ, Carlone RL. The Endocannabinoid System and Invertebrate Neurodevelopment and Regeneration. *Int J Mol Sci*. 2021 Feb 20;22(4):2103.
39. Erben L, Buonanno A. Detection and Quantification of Multiple RNA Sequences Using Emerging Ultrasensitive Fluorescent In Situ Hybridization Techniques. *Curr Protoc Neurosci*. 2019 Apr;87(1):e63.
40. Tao R, Li C, Jaffe AE, Shin JH, Deep-Soboslay A, Yamin R, et al. Cannabinoid receptor CNR1 expression and DNA methylation in human prefrontal cortex, hippocampus and caudate in brain development and schizophrenia. *Transl Psychiatry*. 2020 May 19;10(1):158.
41. Steindel F, Lerner R, Häring M, Ruehle S, Marsicano G, Lutz B, et al. Neuron-type specific cannabinoid-mediated G protein signalling in mouse hippocampus. *J Neurochem*. 2013 Mar;124(6):795–807.
42. Tzounopoulos T, Kraus N. Learning to encode timing: mechanisms of plasticity in the auditory brainstem. *Neuron*. 2009 May 28;62(4):463–9.
43. L M, L G, D C, Oj M. Altered surface trafficking of presynaptic cannabinoid type 1 receptor in and out synaptic terminals parallels receptor desensitization. *Proceedings of the National Academy of Sciences of the United States of America* [Internet]. 2008 Nov 25 [cited 2024 Oct 12];105(47). Available from: <https://pubmed.ncbi.nlm.nih.gov/19015531/>
44. Li H, Yang J, Tian C, Diao M, Wang Q, Zhao S, et al. Organized cannabinoid receptor distribution in neurons revealed by super-resolution fluorescence imaging. *Nat Commun*. 2020 Nov 11;11(1):5699.
45. Stella N. Cannabinoid and cannabinoid-like receptors in microglia, astrocytes, and astrocytomas. *Glia*. 2010 Jul;58(9):1017–30.
46. Fernández-Moncada I, Marsicano G. Astroglial CB1 receptors, energy metabolism, and gliotransmission: an integrated signaling system? *Essays Biochem*. 2023 Mar 3;67(1):49–61.
47. Oliveira da Cruz JF, Robin LM, Drago F, Marsicano G, Metna-Laurent M. Astroglial type-1 cannabinoid receptor (CB1): A new player in the tripartite synapse. *Neuroscience*. 2016 May 26;323:35–42.

**Figure 1. Distribution analysis of CB1 in central auditory nuclei.**

**(a) Immunostaining of CB1 within auditory center from  $Cnr1^{flox/flox}$ .** The expression of CB1 receptors in different auditory nuclei were demonstrated by fluorescence signals. CN, cochlear nucleus; SOC, superior olivary complex; LL, lateral lemniscus; IC, inferior colliculus; MGB, medial geniculate body; AC, auditory cortex. **(b)(c) Numbers of CB1 positive neurons and average fluorescence intensities of CB1 proteins.** The number of CB1<sup>+</sup> neurons within distinct nuclei were counted manually, and the average intensity of the fluorescence signal was integrated for each nucleus from  $Cnr1^{flox/flox}$ .

**Figure 2. CB1 expression patterns in subregions of central auditory nuclei.**

**(a) Immunostaining of CB1 within subregions of auditory nuclei from the transgenic mice  $Cnr1^{flox/flox}$ .** The auditory nuclei of CN, SOC, and IC with their fundamental subregions were shown in detailed. DCN, dorsal cochlear nucleus; AVCN, anterior ventral cochlear nucleus; PVCN, posterior ventral cochlear nucleus; MSO, medial superior olive; LSO, lateral superior olive; MNTB, medial nucleus of the trapezoid body; ECIC, external cortex inferior colliculus; DCIC, dorsal cortex inferior colliculus; CNIC, central nucleus inferior colliculus. **(b) Numbers of CB1 positive neurons and average fluorescence intensities of CB1 proteins.** The number of CB1<sup>+</sup> neurons within these subregions were counted manually, and the average intensity of the fluorescence signal was integrated for each subregion of CN, SOC, and IC from  $Cnr1^{flox/flox}$ . Data presented as means  $\pm$  SEM. \* $p < 0.05$ , \*\* $p < 0.01$ , \*\*\*\* $p < 0.0001$ .

**Figure 3. CB1R knockout decreases the distribution of CB1R<sup>+</sup> PV-neurons.**

**(a) Double-staining of PV and CB1.** The immunoactivity for PV was shown in red, and CB1 was shown in green. Their co-localization in the regions of CN and SOC was shown in yellow as merged. **(b) Comparison of PV and CB1 expression.** The numbers of PV<sup>+</sup> neurons within CN and SOC were counted manually for each nucleus from  $Cnr1^{flox/flox}$ , and they were compared with PV-Cre; $Cnr1^{flox/flox}$ . So as the analysis of CB1<sup>+</sup> neurons. Data presented as means  $\pm$  SEM. \* $p < 0.05$ , \*\* $p < 0.01$ , \*\*\*\* $p < 0.0001$ . **(c) Co-localization analysis of PV and CB1 in CN or SOC.** Ratios of distinct PV<sup>+</sup> neurons were calculated according to the cell with CB1 expressed in or not.

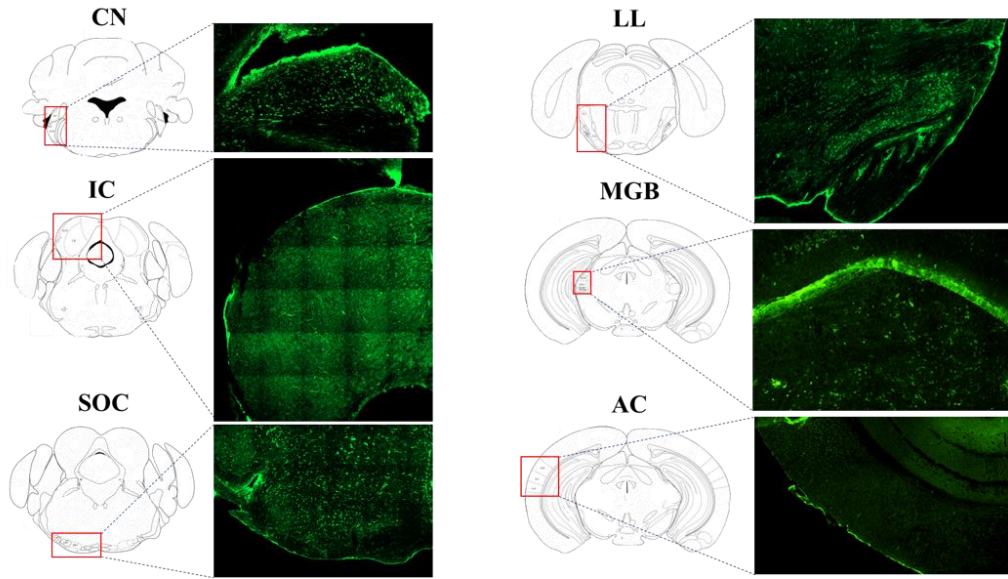
**Figure 4. PV-Cre; $Cnr1^{flox/flox}$  mice exhibit partial hearing loss and abnormal auditory brainstem responses.**

**(a) The waveforms of ABR test.** The waveforms derived from ABR data were collected under click and tone burst stimulus of 16 kHz respectively. The black line represented non-KO mice  $Cnr1^{flox/flox}$ , and the red line represented PV-Cre; $Cnr1^{flox/flox}$  mice. **(b) The hearing thresholds obtained from ABR waveforms.** The hearing thresholds for each mouse that was recorded under click and pure-tone with five frequencies (4~32 kHz) were analyzed from their ABR waveforms. **(c) Superimposition of ABR waveforms.** The ABR waveforms at 90 dB SPL under click and tone burst stimulus of 16 kHz were superimposed to show the discrepancy of amplitude and latency for wave I~V between two transgenic mice. **(d) The latency and (e) amplitude obtained from ABR waveforms.** The latency and amplitude for each wave was calculated from ABR data collected at 90 dB SPL under 16 kHz, and the amplitudes from data

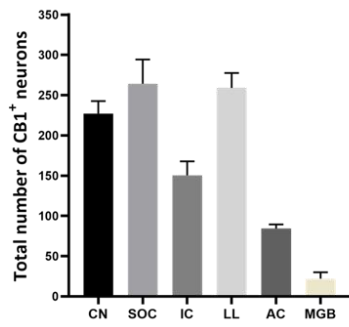
collected at 90 dB SPL under click were also presented. Data presented as means  $\pm$  SEM. \* $p$  < 0.05, \*\* $p$  < 0.01, \*\*\* $p$  < 0.0001.

Figure. 1

(a)



(b)



(c)

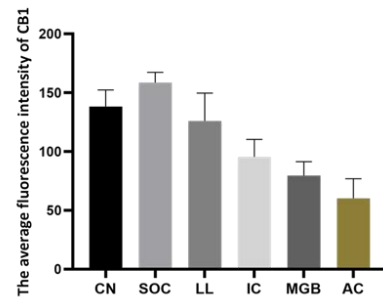
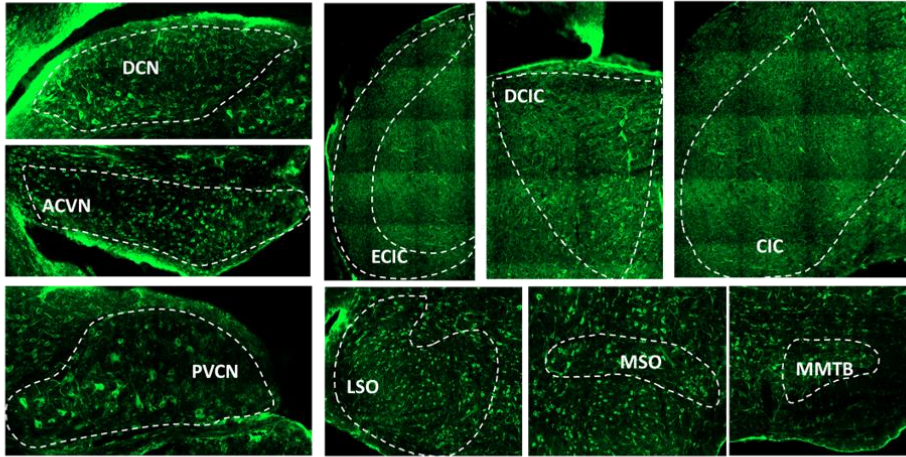
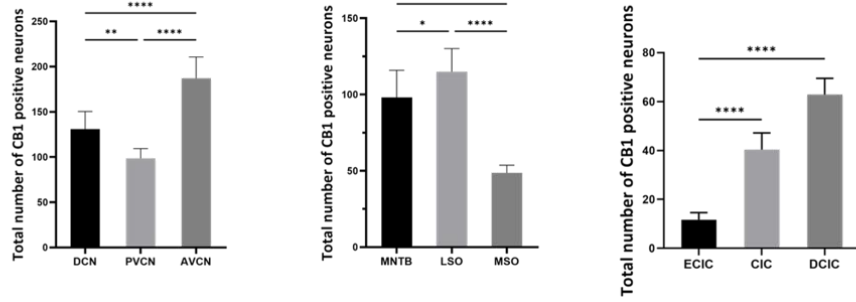


Figure. 2

(a)



(b)



(c)

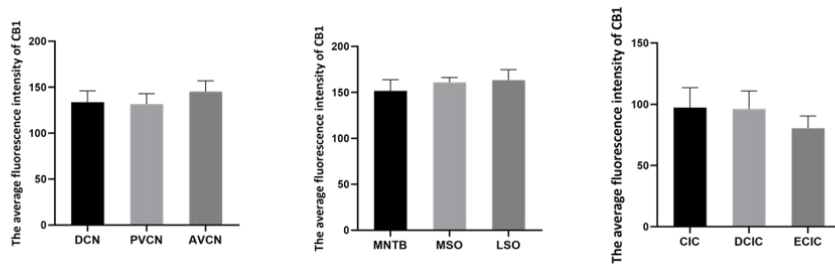
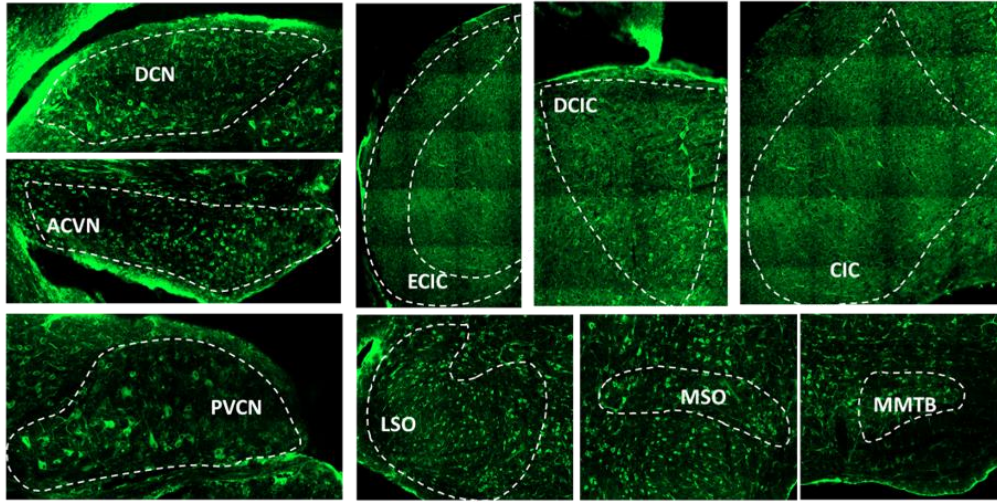
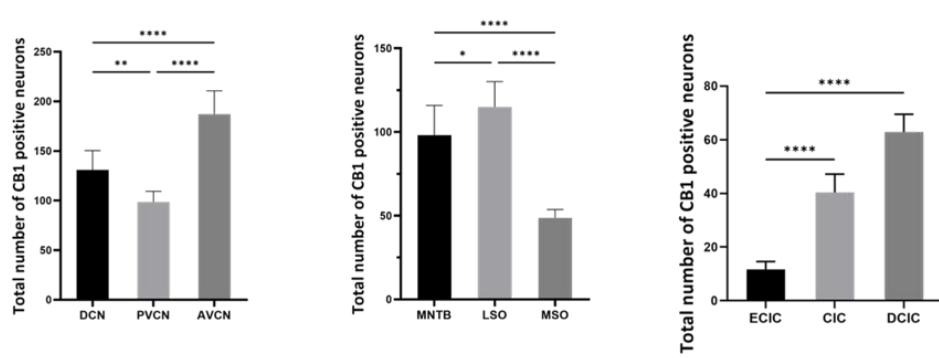


Figure. 3

(a)



(b)



(c)

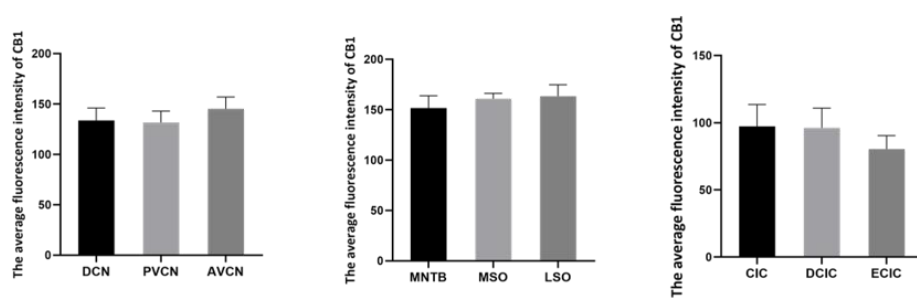


**Figure. 4**

